STUDY OF TRANSIENT BEHAVIOR OF FINNED COIL HEAT EXCHANGERS

S.P. Rooke and M.G. Elissa
Department of Mechanical Engineering
The University of Akron
Akron, OH. 44325-3903

SUMMARY

The status of research on the transient behavior of finned coil cross-flow heat exchangers using single phase fluids is reviewed. Applications with available analytical or numerical solutions are discussed. Investigation of water-to-air type cross-flow finned tube heat exchangers is examined through the use of simplified governing equations and an up-wind finite difference scheme. The degenerate case of zero air-side capacitance rate is compared with available exact solution. Generalization of the numerical model is discussed for application to multi-row multi-circuit heat exchangers.

INTRODUCTION

Significant activity has occurred over the last 25 years in the study of the dynamic behavior of heat exchangers. Analytical and numerical solutions of a variety of heat exchanger geometries and applications have appeared. The focus here is specifically with respect to cross-flow heat exchangers for application in the HVAC (and automotive) areas; where geometries are significantly smaller than found in power generation and process industries.

In-depth study of the dynamic behavior of such heat exchangers commenced in the mid-sixties through research aimed at improving dynamic control capabilities of air heating and cooling systems. Numerous simplified first-order transfer function models emerged, such as for bare single tubes in cross flow (refs. 1,2), single pass finned tubes, (ref. 3), serpentine single row (refs. 4,5,6 to 10), and multi-pass cross-counter and cross-parallel flow (refs. 11,12) heat exchangers. Large multi-pass and shell and tube heat exchanger dynamics are discussed in refs. 13 and 14. These references apply to one fluid mixed, liquid to gas cross flow heat exchangers. Most of the results presented are in gain and time constant / frequency response format most useful for control engineering. The aim of all of the above mentioned work was to derive transfer functions relating outlet temperature response of the primary and secondary fluids to changes in flow rate or temperatures of the inlet conditions of primary or secondary fluids. Each of the above references provide up to 4 transfer functions relating the responses of the outlet temperatures to changes in the inlet flow rates and temperatures. Ref. 15 provides for 6 transfer functions, accounting for primary and secondary fluid temperatures and primary fluid flow rate effects on the outlet temperatures. Ref. 16 provides for 8 transfer functions, including the effects of secondary fluid inlet flow rate on the outlet temperatures. Models are also available which include closed-loop feed back analysis of heat exchanger transients (ref. 17) and heating and cooling system simulation (ref. 18).

Most of the above works account for the presence of external fins, but do so by "lumping" the thermal mass of fins with the tubing, thus neglecting thermal diffusion lags due

to conduction in the fins. Work by Waede Hansen and Demandt (ref. 19) and Kabelac (ref. 20) explores distributed effects of heat diffusion in the fins on the overall response of finned tube heat exchangers. Waede Hansen and Demandt concluded that neglecting heat diffusion effects in the fins was reasonable in the frequency range up to 10-15 rads/sec. Kabelac achieved good agreement with experiment using a model which incorporated fin diffusion effects, but did not separate the effects of the fins from the overall model behavior.

Many of the more rigorous analytic and numerical approaches for transient heat exchanger analysis have been developed more recently and have results presented in temperature vs. time format (i.e. the focus is on heat transfer behavior). Some of these studies are more applicable to a wider class of crossflow heat exchangers (i.e. plate heat exchangers, rod bundles, etc.). Rizika (ref. 21) analytically examined a tube in a constant temperature or insulated environment. Evans and Smith (ref. 22) analytically investigated single pass cross flow heat exchangers with neither fluid mixed, but did not include the effects of metal or matrix thermal capacitance. Myers et al. (refs. 23,24) developed an approximate integral method for single row, single pass geometry (solutions developed for both fluids unmixed). Myers et al. (ref. 25) numerically investigated the case of one fluid having an infinite capacitance rate. Jang and Wang (ref. 26) numerically investigated the case of one fluid mixed. Terasaka et al. (ref. 27) used an approximate method of weighted residuals to investigate the case of both fluids unmixed, neglecting metal/matrix capacitance. Spiga and Spiga (ref. 28) utilized the Laplace transform technique (and numerical inversion) to investigate the case of both fluids unmixed, with metal/matrix capacitance incorporated. Gvozdenac (ref. 29), Spiga and Spiga (ref. 28), Romie (ref. 31), and Chen and Chen (ref. 32) used similar Laplace transform approaches to derive analytical solutions for gas-to-gas, neither fluid mixed geometries. Yamashita et al. (ref. 33) used a finite difference technique to numerically investigate heat exchanger transients with both fluids unmixed. Chiang et al. (ref. 34) numerically investigated a cross counter flow automotive application. Numerical investigation of multi-row cooling coils with condensation occurring on the fins has been studied by Reichert et. al (ref. 35).

While significant effort in the above works have been applied to developing analytical solution techniques and presenting the general transient behavior of the broad class of cross flow heat exchangers, less emphasis has been applied to quantifying behavior of particular applications and circuiting arrangements. Numerical analysis remains the strongest and most flexible technique for examining heat exchanger transients. In the same vein as the work of Myers et al. (ref. 23,24, analytical) and Reichert et al. (ref. 35, numerical, cooling coils), the present study further examines the analysis, mathematical/numerical description, and behavior of heat exchangers for air heating in HVAC.

MATHEMATICAL DEVELOPMENT

A length of finned tube exposed to air in crossflow is to be modelled. The tube could be coiled in serpentine manner, laying in a plane which is perpendicular to the external fluid flow, or it could be a single length of tube in cross flow. Situations where multi-row or parallel/counter cross flow circuiting is employed will be discussed later. The following assumptions will be applied:

1. Incompressible flow.
2. "Plug flow" model for water.
3. Convective coefficients constant during transients, equivalent to steady values.
4. Negligible axial conduction in tube and fluids.
5. Negligible radiative effects.
6. Fins/tube are at one unique temperature at a given x location ("lumped thermal mass").
7. The temperature difference between the tube/fin surface and the air is the logarithmic mean temperature difference.
8. Negligible thermal storage in the air.

The primary fluid (water) is treated as mixed (no variation in temperature except in the flow direction) and the secondary fluid (air) is treated as unmixed (variations in temperature both in the flow direction and normal to the flow direction).

Energy balances on an elemental unit of fin/tube (m), water (w), and air (a) gives the governing equations in the primitive variable form:

$$\left(\rho_t c_{p_t} \vartheta_t' + \rho_f c_{p_f} \vartheta_f'\right)\frac{\partial T_m}{\partial t} - \bar{h}_w P\left(T_w - T_m\right) + \rho_a V_a A_a' c_{p_a}\left(T_{ao} - T_{ai}\right) = 0 \tag{1}$$

$$\rho_w c_{p_w} A_w \frac{\partial T_w}{\partial t} + \rho_w A_w V_w c_{p_w} \frac{\partial T_w}{\partial x} + \bar{h}_w P\left(T_w - T_m\right) = 0 \tag{2}$$

$$\rho_a V_a A_a' c_{p_a}\left(T_{ao} - T_{ai}\right) = \eta_o \bar{h}_a A' LMTD \tag{3}$$

As will be shown later, this form may be of most usefulness for studying individual effects of physical parameters. The case to be studied here will be for the secondary fluid (air) being heated. Thus, temperatures are non-dimensionalized according to $(T-T_{ai})/(T_{wi}-T_{ai})$. Substitution and rearranging gives:

$$\left(\rho_t c_{p_t} \vartheta_t' + \rho_f c_{p_f} \vartheta_f'\right)\frac{\partial \theta_m}{\partial t} - \bar{h}_w P\left(\theta_w - \theta_m\right) + \dot{m}_a' c_{p_a} \theta_{ao} = 0 \tag{4}$$

$$\rho_w c_{p_w} A_w \frac{\partial \theta_w}{\partial t} + \dot{m}_w c_{p_w} \frac{\partial \theta_w}{\partial x} + \bar{h}_w P\left(\theta_w - \theta_m\right) = 0 \tag{5}$$

$$\theta_{ao} = \left[1. - \exp\left(-\eta_o \bar{h}_a A' / \dot{m}_a' c_{p_a}\right)\right]\theta_m \tag{6}$$

To reduce the number of variables, dimensionless groupings as follows are helpful:

$$\chi = x/L \;,\quad \tau = tV_w/L$$
$$N_w = \bar{h}_w PL/\dot{m}_w c_{p_w}$$
$$N_a = \eta_o \bar{h}_a A'/\dot{m}_a' c_{p_a}$$
$$C_r = C_m/C_w$$
$$H_r = \eta_o \bar{h}_a A'/\bar{h}_w P$$

Insertion into the governing equations produces

$$\frac{\partial \theta_m}{\partial \tau} + \frac{N_w}{C_r}(\theta_m - \theta_w) + \frac{N_w H_r}{N_a C_r}\theta_{ao} = 0 \tag{7}$$

$$\frac{\partial \theta_w}{\partial \tau} + \frac{\partial \theta_w}{\partial \chi} + N_w(\theta_w - \theta_m) = 0 \tag{8}$$

$$\theta_{ao} = \left[1 - \exp(-N_a)\right]\theta_m \tag{9}$$

Substitution of Eqn.(9) into Eqns. (7) and (8) yields

$$\frac{\partial \theta_{ao}}{\partial \tau} + \left[\frac{N_w}{C_r} + \frac{f(N_a)N_w H_r}{N_a C_r}\right]\theta_{ao} - \left[\frac{f(N_a)N_w}{C_r}\right]\theta_w = 0 \tag{10}$$

$$\frac{\partial \theta_w}{\partial \tau} + \frac{\partial \theta_w}{\partial \chi} + N_w\theta_w - \frac{N_w}{f(N_a)}\theta_{ao} = 0 \tag{11}$$

where $f(N_a)=1-\exp(-N_a)$. Initially, the primary fluid, metal, and secondary fluid temperatures are at zero. The primary fluid (water) temperature is subject to a sudden step change in temperature. The boundary and initial conditions are then

$$\theta_w(\chi,0) = \theta_{ao}(\chi,0) = 0 \tag{12}$$

$$\theta_w(1,\tau) = 1 \tag{13}$$

The dimensionless groupings are the minimum number required to describe the problem. While $N_w=NTU_w$ and $N_a=NTU_a$ have the same form as the conventional "Number of transfer units", they are not actually NTU values. Conversion of these dimensionless variables used into the conventional NTU (ref. 36) can be accomplished as follows:

$$\text{if } \dot{C}_a < \dot{C}_w, \left[\frac{\dot{C}_a}{\dot{C}_w} = \frac{N_w}{N_a}H_r < 1\right] : \quad NTU = \frac{UA}{\dot{C}_a} = \frac{N_a}{1 + H_r} \tag{14}$$

$$\text{if } \dot{C}_w < \dot{C}_a, \left[\frac{\dot{C}_a}{\dot{C}_w} = \frac{N_w}{N_a}H_r > 1\right] : \quad NTU = \frac{UA}{\dot{C}_w} = \frac{H_r N_w}{1 + H_r} \tag{15}$$

N_a and N_w are chosen instead of NTU because they appear naturally in the governing equations, and effectively separate primary and secondary side fluid effects. N_a dictates how close the air temperature comes to the metal temperature (see eqn.6). N_w contains the water flow length L in it, while N_a does not explicitly contain the water flow length. This is a result of the energy equation for the air being lumped and not distributed; thus no characteristic length appears explicitly on the air side. Use of the steady state NTU is not straight forward in parametric studies where the definition can vary. N_a and N_w are also used by Spiga and Spiga (ref. 28) and

Chen and Chen (ref. 32). As will be shown, even the non-dimensional parameters selected do not allow for a perfect separation of all fluid and heat transfer effects. For example, variations in air side resistance affect both the N_a as well as H_r. This duplicity cannot be avoided however, even with a different selection of non-dimensional parameters.

NUMERICAL TECHNIQUE

A forward time backward space finite difference scheme was chosen for the numerical calculations. The explicit formulation was chosen as a "first cut" approach. Eqns. (10) and (11) become

$$\theta_{ao,i}^{n+1} = \left[1 - \frac{N_w \Delta\tau}{C_r} - \frac{f(N_a) N_w H_r \Delta\tau}{N_a C_r}\right] \theta_{ao,i}^{n} + \left[\frac{f(N_a) N_w \Delta\tau}{C_r}\right] \theta_{w,i}^{n} \tag{16}$$

$$\theta_{w,i}^{n+1} = \left[1 - \frac{\Delta\tau}{\Delta\chi} - N_w \Delta\tau\right] \theta_{w,i}^{n} + \frac{\Delta\tau}{\Delta\chi} \theta_{w,i-1}^{n} - \frac{N_w \Delta\tau}{f(N_a)} \theta_{ao,i}^{n} \tag{17}$$

A stability criteria arising from Eqn.(17) is seen to be

$$\Delta\tau \leq \frac{1}{\frac{1}{\Delta\chi} + N_w} \tag{18}$$

N_w in Eqn.(18) arises from the convection term in Eqn.(11). In a purely advective problem, $N_w=0$ and $\Delta\tau=\Delta\chi$ would result (a desirable result, since in dimensional form it is equivalent to $\Delta t \cdot V_w = \Delta x$, which implies that a fluid front properly arrives at a spacial grid point precisely at the time dictated by the fluid velocity.) In the present work the numerical constraint on $\Delta\tau$ is $\Delta\tau < \Delta\chi$, which implies a fluid front will appear at a given grid point prior to what is physically dictated by the fluid velocity. Note that by writing $\Delta\tau = \phi \cdot \Delta\chi$, where $0 \leq \phi \leq 1$, for best representation of the physics, we want $\phi \approx 1$. We can then methodically select grid spacing according to

$$\Delta\chi = \frac{1 - \phi}{\phi N_w} \tag{19}$$

and as ϕ approaches 1, $\Delta\tau$ approaches $\Delta\chi$. Computational effort increases significantly as this is done.

RESULTS AND DISCUSSION

A parametric study is presented using the above parameter definitions over ranges of the parameters found to cover the design and operation of several manufactured air heating coils as determined by a survey of manufacturer's catalogs and designs reported previously in the literature.

An exact solution for the problem at hand is not available. However, Myers et al. (ref. 37) provide an analytic solution for the degenerate case of zero air side capacitance rate. This idealized situation was simulated in the present case by forcing N_a to be very large.

Fig. 1 provides a comparison between the numerical model and the exact solution for the case of negligible air side capacitance. Fig. 1 illustrates a severe test of the numerical model, that of correctly predicting the step response of the primary fluid (water) at the outlet, at a water flush time of one. The comparison is seen to improve as the value of ϕ in Eqn. 19 approaches 1.0 (i.e. decreasing grid and time spacings). A reasonable trade-off between accuracy required for this study and computational effort was to keep ϕ in the neighborhood of 0.995. Figure 2 illustrates that the ϕ criteria has a less dramatic effect on the secondary side fluid (air). For a fixed ϕ less than 1.0, error in temperature is approximately constant versus time, although the magnitude of temperature increases with time and the error appears larger at longer times. The ability to control numerical error is demonstrated; however, since numerically the $\phi \neq 1$ implies some error, the explicit formulation is not particularly attractive on this point and future studies should explore implicit techniques.

Figures 3 and 4 reflect the effects of the metal to water capacitance ratio on outlet water and air temperatures, respectively. The value of C_r does not effect the steady state values of the dimensionless temperatures, but has a strong influence on the transient behavior as expected. Response times can be compared directly between each of the curves on either figure, with greater response times obtained for larger C_r (larger wall capacitance).

Transient heat exchanger efficiency is a useful parameter which compares the energy leaving the heat exchanger via the air stream to the energy that is given up by the water stream, at a given instant during the transient. At steady state, the efficiency will equal one. For heating of the air, we define the transient efficiency as:

$$\textit{Transient Efficiency},\ \epsilon = \frac{(\dot{m}c_p)_a\,(T_{ao} - T_{ai})}{(\dot{m}c_p)_w\,(T_{wi} - T_{wo})}$$

Figure 5 reflects the transient efficiency versus time for the case of varying capacitance ratio. Discontinuities in the curves appear at a dimensionless time of one due to the fact that the water outlet temperature changes abruptly at one flush time. While discontinuities are not an attractive feature for performance diagrams, this is a reflection of what is really occurring. The transient efficiency plot also allows us to compare overall heat exchanger response times for different values of the parameter being studied.

Figures 6 and 7 show the dependence of outlet water and air temperature on N_a, respectively. One can view the N_a variation as a variation in the air flow rate, with smaller N_a values reflecting larger air mass flow rates (with the air side resistance artificially held fixed). As N_a decreases, the water outlet temperature, and hence the air outlet temperature, are seen to decrease. Figure 8 depicts the transient efficiency from which overall response times may be compared. Comparisons of Figs. 6,7, and 8 demonstrate the utility of presenting both outlet temperatures and efficiency; while response time is enhanced by increasing the air mass flow rate (decrease in N_a), one would not want to maximize air mass flow rate in most designs because by doing so the air experiences a negligible rise in temperature.

The effect of the length of the heat exchanger is examined with the N_w parameter. Figs. 9

and 10 show the outlet water and air temperatures, respectively versus the dimensionless time with N_w as a parameter. The x-axis is normalized with respect to the flush time of the water of the $N_w=1$ case so that time durations are equivalent between the different N_w curves. Thus, one flush time is shown at $Tau^*=1$ for the $N_w=1$ case, while for the $N_w=8$ case, the flush time occurs at $Tau^*=8$ since its length is 8 times longer than for $N_w=1$ (assuming the same fluid velocity in each case). As N_w decreases, the outlet water temperature approaches the inlet water temperature, the outlet air temperature approaches the water temperature, and steady state is reached more quickly than for the larger values of N_w. The transient efficiency curves shown in Fig. 11 more directly compare response time for the N_w variations. Note that $N_w=1,4$, and 8 correspond to the conventional units of NTU=0.5, 2.0, and 4.0, respectively, here.

Approximate solutions are available for the cases examined here. The current work is not intended to replace previously available solutions, but rather to complement them. Effort has been aimed at outlining and describing the results and limitations of a simplified numerical solution approach to solve for heat exchanger transients.

Extension of the current work is ongoing to further utilize the flexibility of the numerical approach. Areas being studied include examining the effects of tube rows on transient behavior and examining changes in secondary fluid temperatures and the flow rates of both fluids. Comparisons of solutions between the present modeling approach and a simplified model using ordinary differential equations is also underway. It is anticipated that these efforts will add further insight into modeling requirements as well as insight into design of heat exchangers with consideration of transients.

Acknowledgements

Financial support for this research received from the Ohio Board of Regents Research Challenge Grant (ORSSP#R2444) and from the Faculty Projects Research Committee of the University of Akron (FRG#1244) is gratefully acknowledged.

NOMENCLATURE

A	Area (m^2)
c_p	Specific heat (J/kg·K)
C_r	Dimensionless ratio of metal capacitance to water capacitance.
$\dot{C}$	Capacitance rate (W/K), mass flow specific heat product.
h	Convective heat transfer coefficient ($W/m^2 \cdot K$)
H_r	Dimensionless ratio of water side resistance to air side resistance.
L	Total flow length experienced by water (m)
LMTD	Logarithmic mean temperature difference: $(T_{ao}-T_{ai})/\ln[(T_m-T_{ai})/(T_m-T_{ao})]$
$\dot{m}$	Mass flow rate (kg/s)
NTU	Number of transfer units, $UA/\dot{C}_{min}$.
N_w	(NTU_w) Dimensionless number, inverse of water side resistance-capacitance product.
N_a	(NTU_a) Dimensionless number, inverse of air side resistance-capacitance product.
P	Tube inner perimeter (m)

t	Time (s)
UA	Overall heat transfer coefficient (W/K)
V	Velocity (m/s)
ϑ	Volume (m^3)
x	Axial position along tube (m)

greek

ρ	Density (kg/m^3).
η	Surface efficiency
τ	Dimensionless time, tV_w/L.
θ	Dimensionless temperature $(T-T_{ai})/(T_{wi}-T_{ai})$
χ	Dimensionless position, x/L.

subscripts		superscripts	
w	water	n	time level
a	air	′	per unit length
ai	inlet air	–	length or surface averaged
ao	outlet air		
i	grid point		
m	metal (fin plus tubing)		
f	fin		
t	tube		

REFERENCES

1. Gartner, J.R.; and Harrison, H.L.: Frequency Response Transfer Function for a Tube in Crossflow. ASHRAE Trans., vol. 69, 1963, pp. 323-330.
2. McNamara, R.T.; and Harrison, H.L.: A Lumped Parameter Approach to Crossflow Heat Exchanger Dynamics. ASHRAE Trans., vol.73, pt.2, 1967, pp. iv.1.1-iv.1.9.
3. Gartner, J.R.; and Harrison, H.L.: Dynamic Characteristics of Water-to-Air Crossflow Heat Exchangers. ASHRAE Trans., vol. 71, pt.1, 1965, pp. 212-224.
4. Tobias, J.R.: Simplified Transfer Function for Temperature Response of Fluids Flowing Through Coils, Pipes or Ducts. ASHRAE Trans., vol. 79, pt.2, 1973, pp. 19-22.
5. Gartner, J.R.: Simplified Dynamic Response Relations for Finned-Coil Heat Exchangers. ASHRAE Trans., vol. 76, pt.2, 1972, pp. 163-169.
6. Gartner, J.R.; and Daane, L.E.: Dynamic Response Relations for a Serpentine Crossflow Heat Exchanger with Water Velocity Disturbance. AHSRAE Trans., vol.75, pt.1, 1969, pp. 53-68.
7. Pearson, J.T.; Leonard, R.G.; McCutchan, R.D.: Gain and Time Constant for Finned Serpentine Crossflow Heat Exchangers. ASHRAE Trans., vol. 80, pt.2, 1974, pp. 255-267.
8. Boot, J.L.; Pearson, J.T.; Leonard, R.G.: An Improved Dynamic Response Model for Finned Serpentine Cross-Flow Heat Exchangers. ASHRAE Trans., vol. 84, pt. 1, 1977, pp. 218-239.

9. Jawadi, Z.: A Simple Transient Heating Coil Model. In Analysis of Time-Dependent Thermal Systems, AES-vol.5, Wepfer, W.J.; Klein, S.A.; Patton, J.S. Eds., ASME, New York, 1988, pp. 63-69.
10. Underwood, D.M.; and Crawford, R.R.: Dynamic Nonlinear Modeling of a Hot-Water-to-Air Heat Exchanger for Control Applications. ASHRAE Trans., vol. pt.1, 1991, pp. 149-155.
11. Tamm, H.: Dynamic Response Relations for Multi-Row Crossflow Heat Exchangers. ASHRAE Trans., vol.75, pt.1, 1969, pp. 69-80.
12. Tamm, H.; and Green, G.H.: Experimental Multi-Row Crossflow Heat Exchanger Dynamics. ASHRAE Trans., vol. 79, pt. 2, 1973, pp. 9-18.
13. Williams, T.J.; and Morris, H.J.: A Survey of the Literature on Heat Exchanger Dynamics and Control. Chem. Eng. Symp. Ser. no. 36, vol. 57, 1961, pp. 20-33.
14. Matsuyama, H.; and O'Shima, E.: Representation of Dynamics of Multipass Heat Exchangers. Heat Transfer Japanese Research, Apr.-Jun., 1975, pp. 1-11.
15. Franck, G.: Dynamisches Verhalten von Kreuzstromwärmeübertragern. Wärme und Stoffübertragung, vol. 20, 1986, pp. 141-149.
16. Bender, E.: Dynamic Response of Crossflow Heat Exchangers for Variations in Temperature and Massflow. Proc. of the 5th IFAC World Congress, 1972, pp. 8.3.1-8.3-10.
17. Maxwell, G.M.; Shapiro, H.N.; Westra, D.G.: Dynamics and Control of a Chilled Water Coil. ASHRAE Trans., vol. 1989, pp. 1243-1255.
18. Clark, D.R.; Hurley, C.W.; Hill, C.R.: Dynamic Models for HVAC System Components. ASHRAE Trans., vol. 91, 1985, pp. 737-751.
19. Waede Hansen, K.; Demandt, K.: Dynamics of a Cross-Flow Heat Exchanger with Fins. Int. J. Heat Mass Transfer, vol. 17, 1974, pp. 1029-1036.
20. Kabelac, S.: The Transient Response of Finned Crossflow Heat Exchangers. Int. J. Heat Mass Transfer, vol. 32, no. 5, 1989, pp. 1189-1192.
21. Rizika, J.W.: Thermal Lags in Flowing Incompressible Fluid Systems Containing Heat Capacitors. ASME, New York, 1954, Paper No. 54-SA-50.
22. Evans, F.; and Smith, W.: Cross-Current Transfer Processes in the Non-Steady State. Proc. Roy. Soc., London, vol. 272 A, 1962, pp. 241-269.
23. Myers, G.E.; Mitchell, J.W.; Nagaoka, R.: A Method of Estimating Cross-Flow Heat Exchanger Transients. ASHRAE Trans., vol. 71, pt.1, 1965, pp. 225-230.
24. Myers, G.E.; Mitchell, J.W.; Lindeman, C.F.: The Transient Response of Heat Exchangers Having an Infinite Capacitance Rate Fluid. J. Heat Transfer, May 1970, pp. 269-275.
25. Myers, G.E.; Mitchell, J.W.; and Norman, R.F.: The Transient Response of Crossflow Heat Exchangers, Evaporators, and Condensers. J. Heat Transfer, Feb. 1967, pp. 75-80.
26. Jang, J.Y.; and Wang, M.T.: Transient Response of Crossflow Heat Exchangers with One Fluid Mixed. Heat and Fluid Flow, vol.8, no.3, Sept. 1987, pp. 182-186.
27. Terasaka, H.; Kanoh, H.; Masubuchi, M.: Approximate Dynamic Analysis of Crossflow Heat Exchanger by the Method of Weighted Residuals. Bull. of the JSME, vol.23, no.177, Mar. 1980, pp. 432-438.
28. Spiga, M.; Spiga, G.: Transient Temperature Fields in Crossflow Heat Exchangers With Finite Wall Capacitance. J. Heat Transfer, vol.110, Feb. 1988, pp. 49-53.
29. Gvozdenac, D.D.: Analytical Solution of the Transient Response of Gas-to-Gas Crossflow

Heat Exchanger with Both Fluids Unmixed. J. Heat Transfer, vol. 108, Nov. 1986, pp. 722-727.
30. Spiga, M.; Spiga, G.: Two-Dimensional Transient Solutions for Crossflow Heat Exchangers With Neither Gas Mixed. J. Heat Transfer, vol. 109, 1987, pp. 281-286.
31. Romie, F.E.: Transient Response of Gas-to-Gas Crossflow Heat Exchangers with Neither Gas Mixed. J. Heat Transfer, vol. 105, May 1987, pp. 518-521.
32. Chen, H.T.; and Chen, K.C.: Transient Response of Crossflow Heat Exchangers with Finite Wall Capacitance. J. Heat Transfer, vol.114, Aug. 1992, pp.752-755.
33. Yamashita, H.; Izumi, R.; Yamaguchi, S.: Analysis of the Dynamic Characteristics of Cross-Flow Heat Exchangers With Both Fluids Unmixed (On the Transient Responses to a Step Change in the Inlet Temperature). Bull. of the JSME, vol.21, no.153, Mar. 1978, pp. 479-485.
34. Chiang, E.C.; Chellaiah, S.; Johnson, J.H.: Modeling of Convective Heat Flow in Radiators for Coolant Temperature Prediction. ASME, New York, 1985, paper 85-WA/HT-22.
35. Reichert, B.A.; Nelson, R.M.; Pate, M.B.: A Computer Simulation of a Cross-Flow Heat Exchanger Operating in a Moist Air Environment. Computer Aided Engineering of Energy Systems, vol.2, ASME, New York, 1986, pp. 89-96.
36. Kays, W.M.; and London, A.L.: Compact Heat Exchangers. Third Edition, McGraw-Hill, New York, 1984, pp. 79-101.
37. Myers, G.E.; Mitchell, J.W.; and Norman, R.F.: The Transient Response of Cross-Flow Heat Exchangers with One Fluid Mixed. Report No. MM-3, Department of Mechanical Engineering, The University of Wisconsin, Madison, Wisconsin, Oct. 1, 1965.

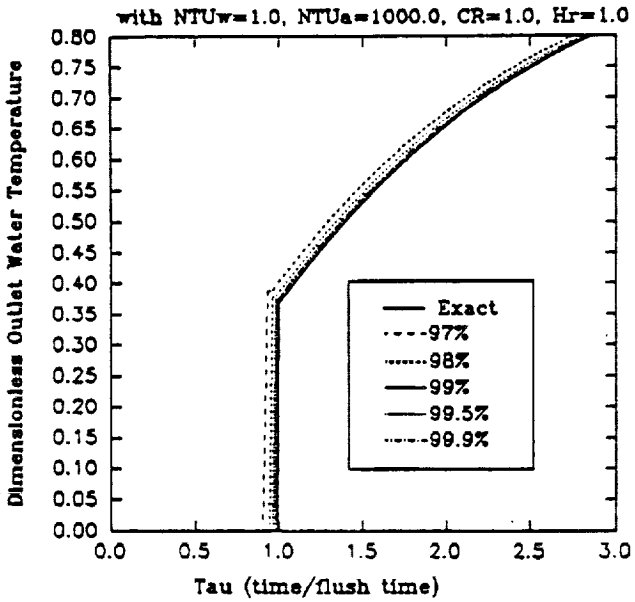

Fig. 1. Comparison of numerical and exact solutions (dimensionless water outlet temperature versus dimensionless time) for the case of negligible air side capacitance, with the grid/time spacing ratio as a parameter.

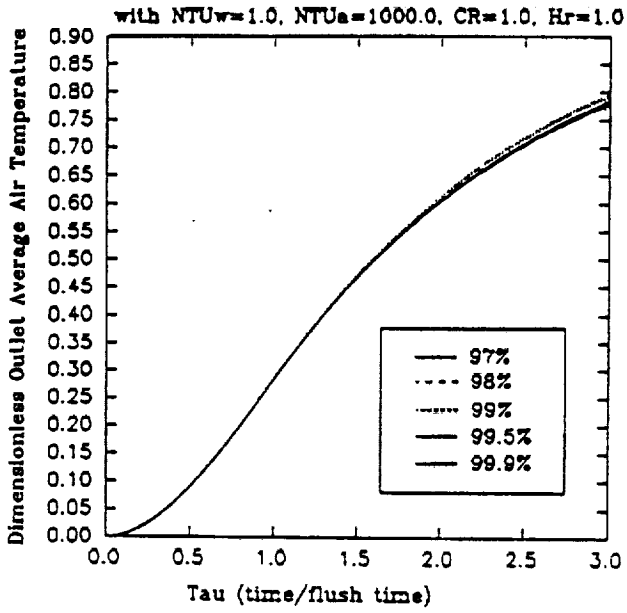

Fig. 2. Comparison of numerical and exact solutions (integrated dimensionless air outlet temperature versus dimensionless time) for the case of negligible air side capacitance, with the grid/time spacing ratio as a parameter.

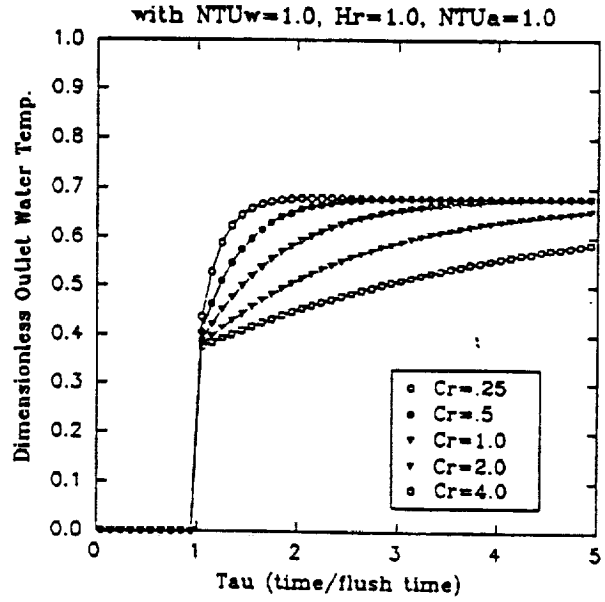

Fig. 3. Dependency of outlet dimensionless water temperature versus dimensionless time on the metal/water capacitance ratio, with all other parameters held fixed.

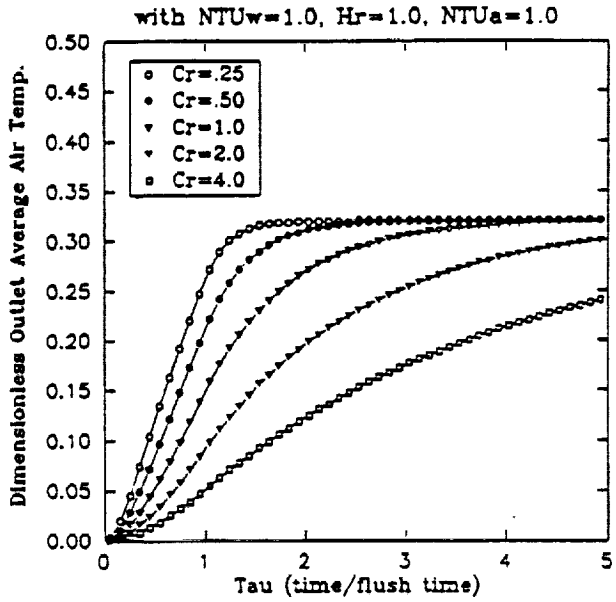

Fig. 4. Dependency of the dimensionless integrated air outlet temperature versus dimensionless time on the metal/water capacitance ratio, with all other parameters held fixed.

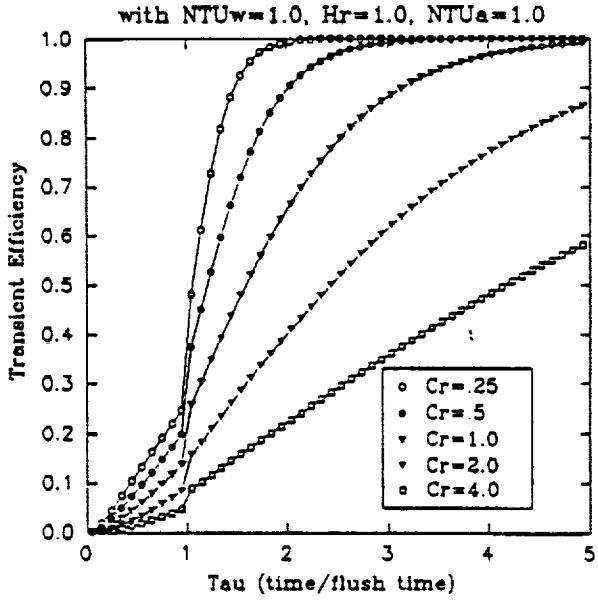

Fig. 5. Dependency of the transient efficiency versus dimensionless time on the metal/water capacitance ratio, with all other parameters held fixed.

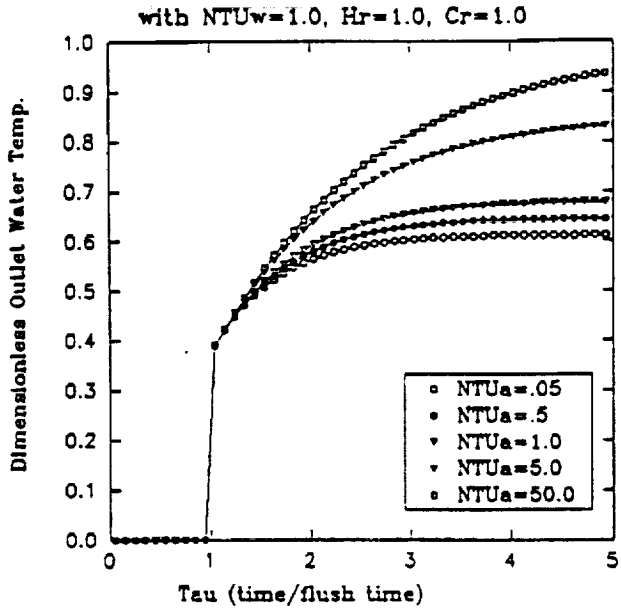

Fig. 6. Dependency of the dimensionless water outlet temperature versus dimensionless time on the N_a parameter, with all other parameters held fixed (simulated air capacitance rate effects).

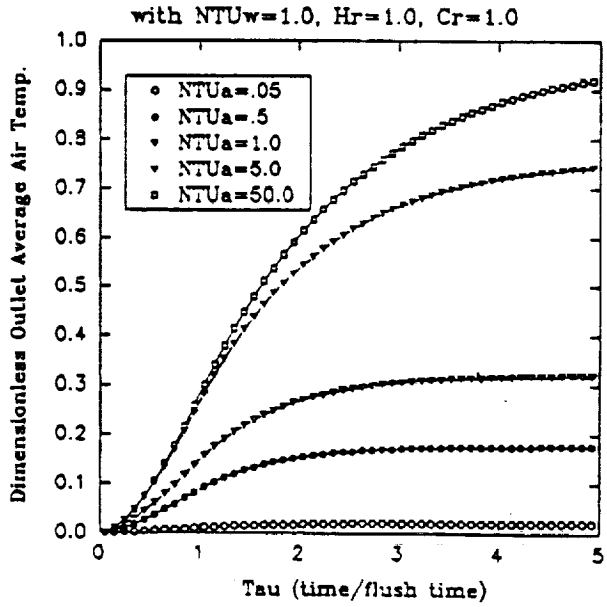

Fig. 7. Dependency of the integrated dimensionless air outlet temperature versus dimensionless time on the N_a parameter, with all other parameters held fixed (simulated air capacitance rate effects).

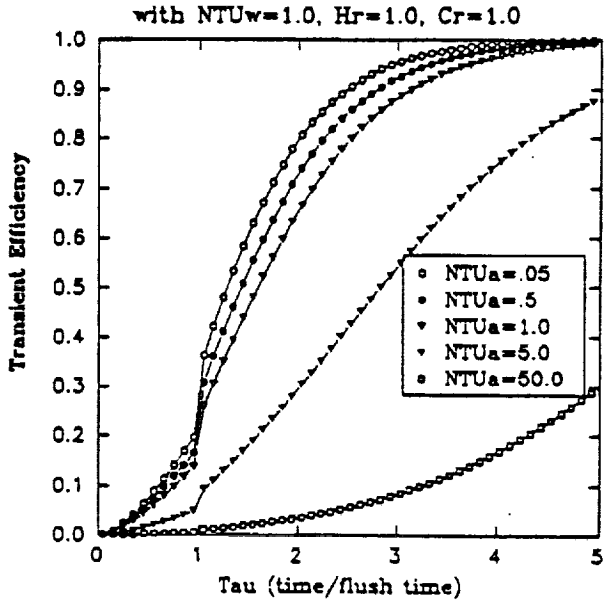

Fig. 8. Dependency of the transient efficiency versus dimensionless time on the N_a parameter, with all other parameters held fixed (simulated air capacitance rate effects).

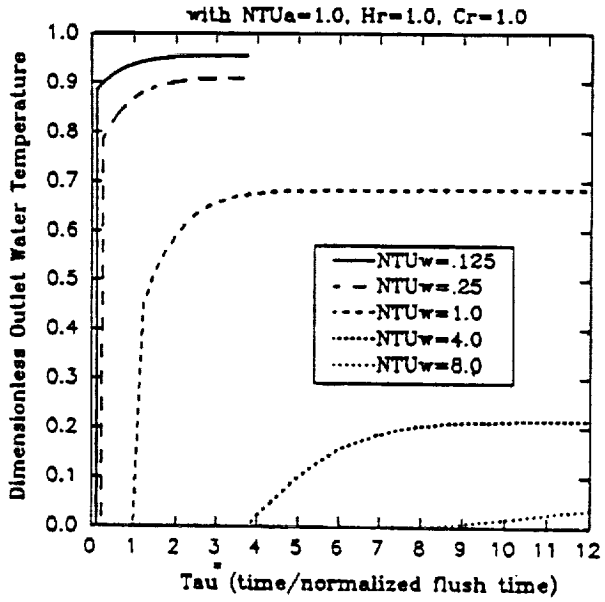

Fig. 9. Dependency of the dimensionless water outlet temperature versus normalized dimensionless time on the N_w parameter, with all other parameters held fixed (simulated heat exchanger length effects).

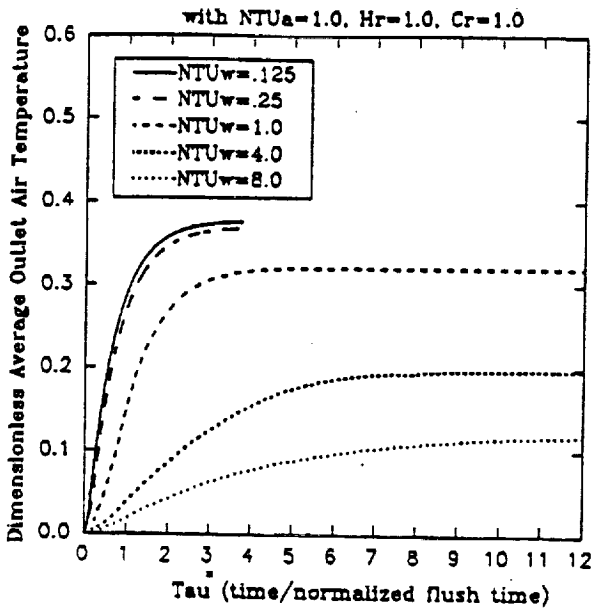

Fig. 10. Dependency of the integrated dimensionless air outlet temperature versus normalized dimensionless time on the N_w parameter, with all other parameters held fixed (simulated heat exchanger length effects).

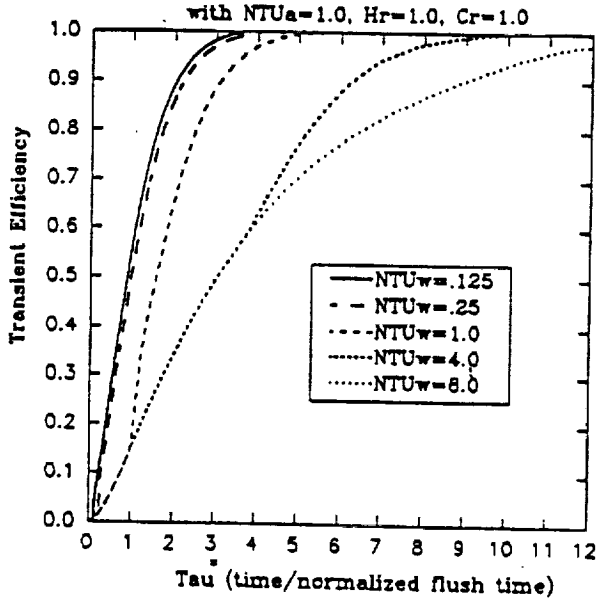

Fig. 11. Dependency of the transient efficiency versus normalized dimensionless time on the N_w parameter, all other parameters held fixed (simulated heat exchanger length effects).